Reactivity of Molecular Oxygen with Aluminum Clusters: Density Functional and *Ab Initio* Molecular Dynamics Simulation Study

Selvarengan Paranthaman,[a,b] Jiwon Moon,[c] Kiryong Hong,[a] Jeongho Kim,[d] Dong Eon Kim,[b,e] Joonghan Kim,*[c] and Tae Kyu Kim*[a]

Dissociative adsorption of molecular oxygen (O_2) on aluminum (Al) clusters has attracted much interest in the field of surface science and catalysis, but theoretical predictions of the reactivity of this reaction in terms of barrier height is still challenging. In this regard, we systematically investigate the reactivity of O_2 with Al clusters using density functional theory (DFT) and atom-centered density matrix propagation (ADMP) simulations. We also calculate potential energy surfaces (PESs) of the reaction between O_2 and Al clusters to estimate the barrier energy of this reaction. The M06-2X functional gives the barrier energy in agreement with the one calculated by coupled cluster singles and doubles with perturbed triples (CCSD(T)) while the TPSSh functional significantly underestimates the barrier height. The ADMP simulation using the M06-2X functional predicts the reactivity of O_2 with the Al cluster in agreement with the experimental findings, that is, singlet O_2 readily reacts with Al clusters but triplet O_2 is less reactive. We found that the ability of a DFT functional to describe the charge transfer appropriately is critical for calculating the barrier energy and the reactivity of the reaction of O_2 with Al clusters. The M06-2X functional is relevant for investigating chemical reactions involving Al and O_2. © 2016 Wiley Periodicals, Inc.

DOI: 10.1002/qua.25080

Introduction

Dissociative adsorption of molecular oxygen (O_2) on aluminum (Al) surface has attracted much interest in the field of surface science and in catalysis.[1–5] In particular, over the past two decades, researchers have made efforts to determine the barrier height of dissociative adsorption of O_2 on Al surfaces both theoretically and experimentally. The calculation of the barrier height using density functional theory (DFT) is one of the most challenging problems in computational chemistry. Previous experimental study on the reaction of O_2 with anionic Al clusters showed that all the Al clusters readily reacts with O_2 in the singlet spin state.[6] In contrast, for O_2 in the triplet spin state, the clusters with an even number of valence electrons do not react.[5] The barrier height can be estimated from molecular beam experiments and was determined to be ~0.3 eV for the dissociative adsorption of O_2 on Al surfaces[7,8] (see Table 1). In contrast, previous DFT studies using generalized gradient approximation (GGA) predicted the absence of any sizeable barrier[11–14] while high-level multireference configuration interaction (MRCI) methods predicted a barrier energy of 0.24 eV.[9] The small barrier heights predicted by the previous DFT studies may be an artifact arising from an improper description of many-body effects in the GGA methods[13] and self-interaction errors of rather old DFT functionals.[10] Meanwhile, Burgert et al. suggested that there is no suitable computational method for calculating the barrier height of O_2/Al reactions.[5]

Recently, there have been many theoretical efforts to calculate barrier heights of the reactions between Al clusters and O_2.[9,10,15–17] For instance, Mosch et al. calculated the barrier height for the dissociative adsorption of O_2 on a model Al surface consisting of neutral Al_4 and Al_{22} clusters and obtained a nonvanishing barrier (<0.1 eV) for the dissociative adsorption of O_2 on Al_{22} clusters using B3LYP with the 6-31G* basis set.[9] Yuan et al. studied the barrier heights for the reactions of Al_7^- and Al_{13}^- with O_2 and suggested that DFT functionals (BLYP, PW91, PBE, B3LYP, and BHHLYP) with the 6-31+G* basis set cannot be used to predict barrier heights.[10] In contrast, highly correlated *ab initio* methods such as coupled-cluster with singles and doubles excitations (CCSD) predicted a

This article was published online on 20 Jan 2016. An error in the name of the fifth author was subsequently identified by the corresponding author. This notice is included in the print and online versions to indicate that both have been corrected on 27 Jan 2016.

[a] *S. Paranthaman, K. Hong, T. K. Kim*
Department of Chemistry and Chemical Institute for Functional Materials, Pusan National University, Busan, 609-735, Republic of Korea
E-mail: tkkim@pusan.ac.kr

[b] *S. Paranthaman, D. E. Kim*
Max Plank Center for Attosecond Science, Pohang 790-784, Republic of Korea

[c] *J. Moon, J. Kim*
Department of Chemistry, the Catholic University of Korea, Bucheon 420-743, Republic of Korea
E-mail: joonghankim@catholic.ac.kr

[d] *J. Kim*
Department of Chemistry, Inha University, Incheon 402-751, Republic of Korea

[e] *D. E. Kim*
Department of Physics and Center for Attosecond Science and Technology, POSTECH, Pohang 790-784, Republic of Korea

Contract grant sponsor: Ministry of Science, ICT & Future Planning (National Research Foundation of Korea (NRF)); contract grant number: NRF-2014R1A1A1007188, 2013R1A1A2009575, 2009-00439, and 2011-0031558.

Table 1. Summary of barrier energies (BE in eV) taken from previous studies.

Refs.	System	Theory or Exp.	BE
Brune et al.[7]	Al (111)+O_2	Molecular beam	~0.3
Mosch et al.[9]	Al_4+O_2	MRCI/TZ	0.24
	Al_{22}+O_2	B3LYP/6-31G*	<0.1
Yuan etal.[10]	Al_7^-+O_2	CCSD/6-31G* //BHHLYP/6-31+G*	0.13
	Al_{13}^-+O_2	CCSD/6-31G* //B3LYP/6-31+G*	0.29
	Al_{13}^-+O_2	CCSD/6-31G* //BHHLYP/6-31+G*	0.25

small barrier (3 kcal/mol = 0.13 eV) when O_2 reacts with Al_7^- clusters.[10] Bacalis et al. used both MRCI and B3LYP methods with the 6-311+G* basis set to predict an activation barrier of 30 kcal/mol for the reaction between O_2 and Al_4 clusters in a total singlet spin state.[17] However, their DFT calculation result was unreasonable because positive charges were localized at an oxygen atom. The lack of consensus among the barrier heights calculated by DFT methods may be attributed to diffuse basis functions or spin states but has not been explained clearly yet. Thus, a systematic theoretical investigation is necessary to clarify this issue.

The main objective of the present work is to clarify the difference in the reactivity of O_2/Al reactions depending on the spin state (singlet vs. triplet) of O_2 using DFT calculation and *ab initio* molecular dynamics (AIMD) simulation. We selected the DFT method as a major tool in this work because DFT is cost-effective and it is not feasible to use high-level *ab initio* methods in the AIMD simulation. As mentioned above, most of DFT functionals were not able to calculate the barrier height of the O_2/Al reactions. In this regard, we also aim to examine whether three recently developed DFT functionals are suitable for describing the interaction between Al clusters and O_2. The success of this work will address why other DFT functionals failed to calculate the barrier energy of O_2/Al reactions and provide a guideline for selecting DFT functionals when studying other similar O_2/Al systems or more realistic systems of O_2 on Al surface.

In the previous theoretical study by Yuan et al.,[10] the Al_{13}^- cluster was employed as a model system for calculating the barrier energy of the reaction between O_2 and Al due to its exceptional stability and structural similarity with the infinitely flat Al(111) surface. However, the AIMD simulation for the Al_{13}^- cluster on various O_2 approaching geometries demands high computational cost and therefore we selected a smaller Al_7^- cluster that is an even-electron system (22 valence electrons) and has a similar three-dimensional structure as Al_{13}^-. To understand the experimental observation of the reactivity between O_2 and Al clusters in terms of reaction pathways, we performed AIMD simulations for the reaction of Al_7^- with O_2 in both singlet and triplet spin states using the atom-centered density matrix propagation (ADMP) method.[18–20] The calculation results presented in this work are in good agreement with the experimentally observed reactivity between O_2 and Al clusters. In addition, for selected molecular configurations of the reactants, potential energy surfaces (PESs) were calculated to estimate the barrier height.

Computational Details

The molecular structures of an isolated Al_7^- cluster, O_2, and reaction products were optimized using M06-2X,[21] TPSSh, (hybrid-meta functionals),[22] and N12-SX[23] (range-separated hybrid nonseparable gradient approximation (NGA)) with the all-electron 6-311+G(d) basis set. Both M06-2X and TPSSh gave reasonable results that agree with previous experimental and high-level theoretical data of Al clusters.[24,25] B3LYP method[26,27] was also used for the comparison with previous studies on the reaction of O_2 with Al clusters.[9,10] Restricted and unrestricted formalisms were employed for the singlet and triplet states, respectively. Harmonic vibrational frequency calculations were performed to identify the minimum energy structure. The PESs were generated to estimate the barrier height by varying the distance between O_2 and Al clusters from 4 to 1 Å with an interval of 0.01Å (see "Calculation of PESs" section). For the calculation of the PESs, we considered the following reactions (the superscripts denote the spin multiplicity):

$$^1Al_7^- + {}^1O_2 \rightarrow {}^1Al_7O_2^- \quad (1)$$

$$^1Al_7^- + {}^3O_2 \rightarrow {}^3Al_7O_2^- \quad (2)$$

Before the reaction starts, in other words, when the distance between Al_7^- and O_2 is large, the triplet spin multiplicity of O_2 has been identified by occupying two α electrons into the molecular orbitals of O_2. Hereafter, except the reaction starting point, the singlet and triplet spin multiplicity means those of whole system (Al_7^-+O_2). The ADMP simulations were carried out up to 400 fs with a time interval of 0.1 fs.[18–20] To reduce the computational cost, we restricted the time range of the ADMP simulation only up to 400 fs. Natural population analyses (NPA) was also performed to examine the charge transfer characteristics between Al clusters and O_2.[28] The coupled cluster singles and doubles with perturbative triples (CCSD(T))/6-311+G(d) calculations[29] were also performed to check the validity of the barrier height calculated by DFT methods. We estimated the barrier height by CCSD(T) via single-point calculations on the top point of rigid scan calculations using M06-2X. The rigid scan means that both the molecular structures of O_2 and Al cluster are frozen (without optimization) during varying the distance between O_2 and Al cluster. In the estimation of the barrier height, the basis set superposition error (BSSE) was corrected. The counterpoise (CP) method[30] was used to consider the BSSE. All calculations were performed using the Gaussian09 program.[31]

Results and Discussion

Selection of DFT functionals

To determine DFT functionals suited for investigating the reactions of Al clusters with O_2, quantum chemical calculations were carried out on two simple model systems, AlO and Al_2O_2, using various DFT functionals such as B3LYP, PBE0, M06-2X, ωB97X, TPSSh, M11, N12-SX, and MN12-SX with the

6-311+G(d) basis set. A recent assessment study[24] and other previous theoretical studies[25] have shown that these functionals can produce the results in agreement with experimental and high-level theoretical investigations on Al clusters. The calculated results are summarized in Supporting Information Table S1 and the optimized molecular structures are shown in Supporting Information Figure S1. As shown in Supporting Information Table S1, the Al−O bond lengths in two electronic states ($^2\Pi$ and $^2\Sigma^+$) of AlO calculated by M06-2X are in close agreement with the experimental values.[32,33] All other functionals slightly overestimated the Al−O bond length and, especially, the B3LYP functional overestimated the Al−O bond length considerably. Regarding the energetic parameters such as the energy difference between the $^2\Pi$ and $^2\Sigma^+$ states of AlO and the vertical ionization energy (vIE) of Al_2O_2, TPSSh, and N12-SX gave reasonably good results in agreement with the experimental values. In particular, the energy difference between the $^2\Pi$ and $^2\Sigma^+$ states (14.1 kcal/mol) calculated by TPSSh is in excellent agreement with the experimental value (14.1 kcal/mol).[34] Although any single DFT functional was not able to accurately predict all the parameters listed in Supporting Information Table S1, three DFT functionals (M06-2X, TPSSh, and N12-SX) gave reasonably good results. Therefore, these three functionals were selected for further investigation of the reactivity of the Al_7^- cluster with O_2. The most commonly used B3LYP functional was also employed for comparison.

Complexes of O_2 and Al cluster. The optimized isolated structures of Al_7^- in both singlet and triplet state are given in Supporting Information Figure S2. The average Al−Al bond length, vertical spin excitation energy, and adiabatic spin excitation energy of Al_7^- and the O−O bond length of O_2 in both singlet and triplet states are also summarized in Supporting Information Table S2. To understand structural changes of the reactant species during the reaction between O_2 and Al_7^-, the geometry optimization was performed for Al_7^- with O_2 in various configurations using M06-2X, TPSSh, N12-SX, and B3LYP functionals. In total, we considered 16 configurations (C1 to C16) shown in Figure 1. In these configurations, the O_2

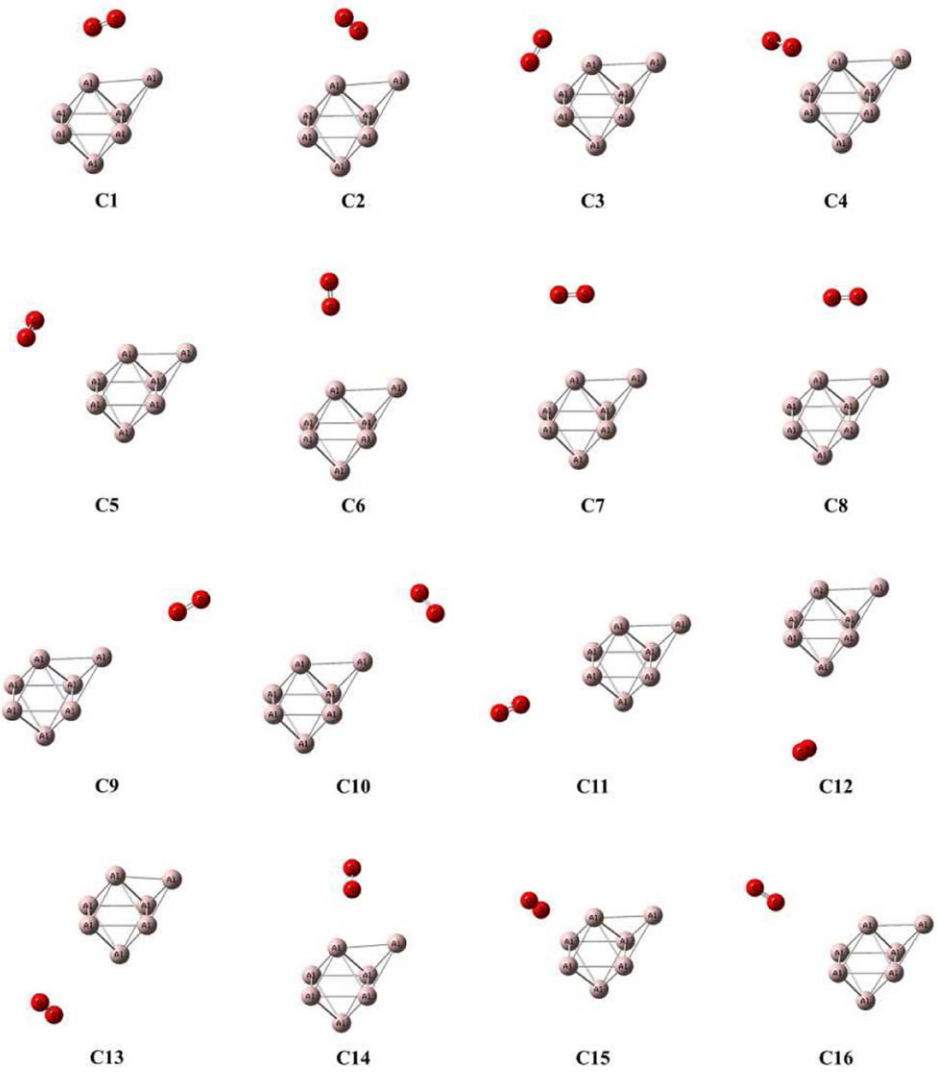

Figure 1. Various configurations of O_2 and Al_7^- considered in this study.

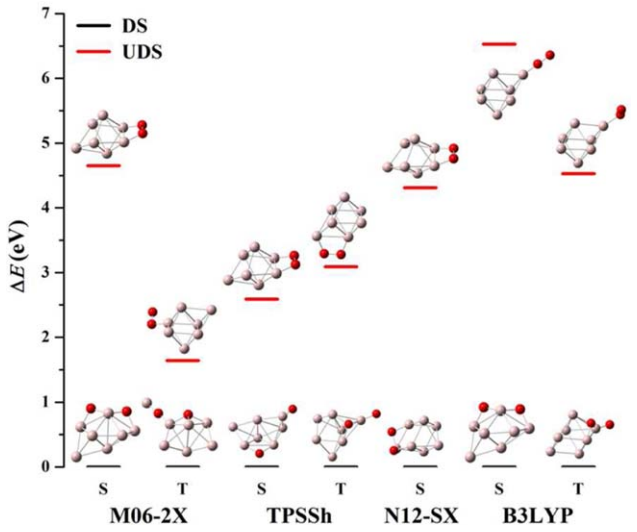

Figure 2. Optimized O−O dissociated structures (DS) and undissociated structures (UDS) formed in the reaction of O_2 with Al_7^-. The S and T mean singlet and triplet, respectively.

molecule was located 2.25 Å from the apex of the Al cluster and the geometry optimizations were performed for both total singlet and triplet spin states. Similar to earlier studies,[9,10] we have considered three adsorption sites on Al cluster for the reaction with O_2 (a) "hollow site" at the center of the triangle of Al_3, (b) "bridge site" between two Al atoms, (c) "top site" direct approach to Al atom both parallel and perpendicular attack of O_2. These optimized structures can be regarded as intermediate structures between the reactants (Al_7^- and O_2) and the products, for example, AlO, AlO_2, and Al_2O. Earlier experimental studies have shown that the above three species are the major products formed in the reaction between Al clusters and O_2 in a cryogenic matrix.[4,5,35,36] Among the 16 configurations, only the optimized structures with the lowest energies were considered for the further discussion. We considered the complexes of O−O dissociated structure (DS) and undissociated structure (UDS), of which the optimized molecular structures and the relative energies are shown in Figure 2.

The DS and UDS complexes can be considered as chemisorbed and physisorbed structures, respectively. In Table 2, we summarized the average bond lengths of the Al−Al, Al−O, and O−O bonds, the total NPA charges localized on the Al cluster and O_2, and the relative energies between DS and UDS structures. According to the calculated results, all the DFT functionals predicted that the DS structures have lower energies than the UDS structures and the DS and UDS complexes have both singlet and triplet states, except the N12-SX functional that gave only the singlet state.

As shown in Table 2, charge transfer occurs from the Al cluster to O_2 for both DS and UDS structures. When comparing the DS and UDS structures, we can see that more charge is transferred in the DS structures than in the UDS structures, resulting in larger negative charge localized on O atoms in the DS structures. These results indicate that charge transfer from the Al cluster to O_2 plays a crucial role in dissociative adsorption of O_2 on the Al cluster. Considering that all the unoccupied molecular orbitals of O_2 are antibonding orbitals (π^* and σ^*), the transferred charge will occupy these orbitals and give rise to the dissociation of O_2. Because the original charge of O_2 is zero, the total charge on O_2 shown in Table 2 corresponds to the transferred charge. The transferred charge values calculated by four DFT functionals are close to 3 in the DS structure, meaning that about three electrons were transferred in the DS structure. Since approximately three electrons are required to dissociate O_2 completely, the charge of less than three on O_2 in the UDS structures leads to the elongation of O–O bond (see Table 2). We note that the TPSSh functional predicted less charge transfer to occur than other DFT functionals, which seems to be related to the underestimation of barrier energy by the TPSSh functional in the following section on the calculation of PESs.

A previous theoretical study employing B3LYP predicted the presence of positive charges localized on O atoms.[17] This unreasonable result could be attributed to the use of Mulliken population analysis (MPA), which shows strong dependence on the basis set. In contrast, all four DFT functionals (M06-2X, TPSSh, N12-SX, and B3LYP) used in the present work successfully described the characteristics of charge transfer, demonstrating the suitability of these functionals for studying the O_2/Al reactions.

Table 2. The average bond lengths of Al−Al bond [r(Al−Al)], Al−O bond [r(Al−O)], O−O bond [r(O−O)], the total NPA charges localized on an Al cluster [q(Al)] and O_2 [q(O)], and the relative energies (ΔE) of dissociated structure (DS) and undissociated structure (UDS) in singlet and triplet states of $Al_7O_2^-$ complexes.

	Singlet		Triplet	
	DS	UDS	DS	UDS
M06-2X				
r(Al−Al) (Å)	2.754	2.678	2.696	2.657
r(Al−O) (Å)	1.742	1.790	1.809	1.840
r(O−O) (Å)	3.009	1.467	2.946	1.322
q(Al)	2.018	0.478	2.209	−0.251
q(O)	−3.018	−1.478	−3.209	−0.749
ΔE (eV)	0.00	4.65	0.00	1.64
TPSSh				
r(Al−Al) (Å)	2.741	2.680	2.712	2.684
r(Al−O) (Å)	1.720	1.812	1.796	1.793
r(O−O) (Å)	5.446	1.510	3.206	1.499
q(Al)	1.759	0.407	1.814	0.404
q(O)	−2.759	−1.407	−2.814	−1.404
ΔE (eV)	0.00	2.59	0.00	3.09
N12-SX				
r(Al−Al) (Å)	2.682	2.659	–	2.628
r(Al−O) (Å)	1.749	1.796	–	1.831
r(O−O) (Å)	2.983	1.469	–	1.325
q(Al)	1.955	0.432	–	−0.259
q(O)	−2.955	−1.432	–	−0.741
ΔE (eV)	0.00	4.31	–	–
B3LYP				
r(Al−Al) (Å)	2.766	2.720	2.791	2.675
r(Al−O) (Å)	1.754	1.653	1.795	1.855
r(O−O) (Å)	3.021	1.384	3.197	1.346
q(Al)	2.003	0.230	1.907	−0.252
q(O)	−3.003	−1.230	−2.907	−0.748
ΔE (eV)	0.00	6.53	0.00	4.53

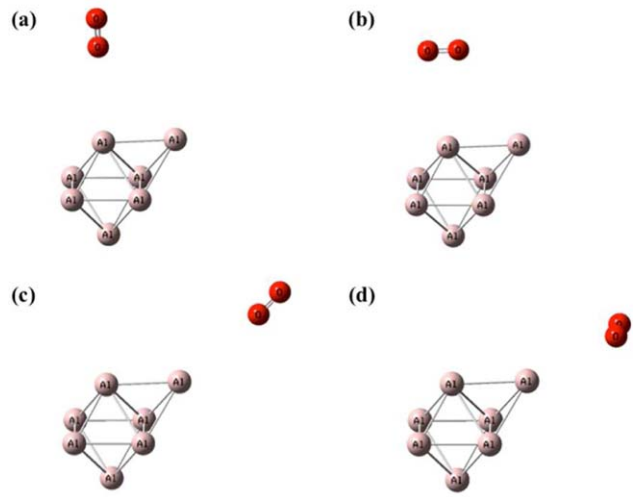

Figure 3. Four configurations of the reaction of O_2 with Al_7^- used in the calculation of PESs. a) O_2 in a parallel orientation approaching from the top of the Al cluster (C6), b) O_2 in a perpendicular orientation approaching from the top of the Al cluster (C7), c) O_2 in a parallel orientation approaching from the side of the Al cluster (C9), and d) O_2 in a perpendicular orientation approaching from the side of the Al cluster (C10).

Calculation of PESs. We performed the calculations of PESs for O_2 approaching the Al_7^- cluster in singlet and triplet spin states to estimate the barrier height of the reaction. We selected four configurations of O_2 and the Al cluster (C6, C7, C9, and C10 in Fig. 1) for the calculation of PESs. The four configurations include (1) O_2 in a parallel orientation approaching from the top of the Al cluster (C6), (2) O_2 in a perpendicular orientation approaching from the top of the Al cluster (C7), (3) O_2 in a parallel orientation approaching from the side of the Al cluster (C9), and (4) O_2 in a perpendicular orientation approaching from the side of the Al cluster (C10). In the parallel orientations (C6 and C9), the distance between Al cluster and O_2 is defined by the distance between marginal Al and O. In the perpendicular orientations (C7 and C10), the distance between Al cluster and O_2 is defined by the distance between marginal Al and the middle point of O_2 using the dummy atom. The selected configurations and the calculated PESs are shown in Figures 3 and 4, respectively. The calculated barrier heights for these four configurations are summarized in Table 3.

We also listed the BSSE corrected barrier height using CP method. As shown in Table 3, the BSSE correction increases the barrier height because the correction on the top point of PES where O_2 is much interacted with Al_7^- larger than that of reactant ($Al_7^- + O_2$). It is well known that the BSSE correction in *ab initio* calculations is larger than that in DFT calculations; the same results are observed in this work. The approach for calculating the barrier energy used in this work is similar to the one used in the previous study by Yuan et al.[10] In that study, the DFT method was not able to predict the barrier height while the CCSD method predicted the barrier height of ~3 kcal/mol ($^3O_2$ approaching an $^1Al_{13}^-$ cluster). In contrast, all the DFT methods successfully predicted the barrier heights of the PESs as can be seen in Figure 4. We found that the barrier height is very small when $^1O_2$ approaches to $^1Al_7^-$ and the barrier height is much larger when $^3O_2$ approaches $^1Al_7^-$ (see Table 3). The BSSE corrected barrier heights also show the same trend; the triplet barrier heights are larger than those of singlet states. Especially, the triplet states calculated by M06-2X show considerably large barrier heights. We note that all DFT functionals used in this work, even B3LYP, gave the barrier heights of a certain amount, which is in contrast to the previous DFT calculations.[9–12,14] The origin of such discrepancy in calculating the barrier energy is not clear yet, but it might be due to the difference in the selected configurations and the size of Al clusters (the effect of diffuse basis function does not alter the results). Therefore, systematic study is necessary to resolve the discrepancy; further investigation on this issue is underway in our group.

As shown in Table 3, only the barrier heights calculated by TPSSh are similar to the experimentally measured value (~ 0.3 eV)[7] for all of the configurations. Based on this result, TPSSh seems to be the best method for calculating the barrier height while M06-2X seems to overestimate the barrier height. However, single-point CCSD(T)/6-311+G(d) calculations gave much larger barrier heights than those from DFT calculations. Therefore, it turns out that all DFT methods, even including M06-2X, underestimate the barrier height and, especially, TPSSh significantly underestimates the barrier height. The underestimation of the barrier height by TPSSh may result from the amount of the charge transfer because the TPSSh functional predicted that less charge is transferred to O_2 than other DFT functionals. In contrast, M06-2X predicted more charge transfer to occur than other DFT functionals, accounting for the larger barrier heights calculated by M06-2X than those calculated by other DFT functionals. Therefore, we conclude that the amount of charge transfer is closely related to the barrier height. In this regard, the ability of a DFT functional to describe the charge transfer appropriately is essential for accurately predicting the barrier height for the reaction between the Al cluster and O_2.

According to these results, all the DFT functionals examined in this work tend to underestimate the barrier height compared with CCSD(T). While M06-2X also underestimates the barrier height, the barrier energies calculated by M06-2X are the closest to the barrier heights estimated by CCSD(T). We can see that the barrier heights calculated by CCSD(T) do not agree with the experimental value, either. The discrepancy might be due to the rigid-scan calculations used in the present work. If the relaxed-scan calculation is used for generating the PESs, CCSD(T) may yield smaller barrier height close to experimental value

ADMP Simulations. For the ADMP simulations, we considered a total of 16 configurations (C1 to C16) of the Al_7^- cluster and O_2 in both singlet and triplet spin states as shown in Figure 1. In all of these configurations, the O_2 molecule was placed 4 Å apart at various positions around the Al_7^- cluster. The O_2-dissociative ADMP trajectories during the reaction of O_2 with Al_7^- are shown in Figure 5 while the nondissociative trajectories are not shown for the sake of clarification. As shown in Figure

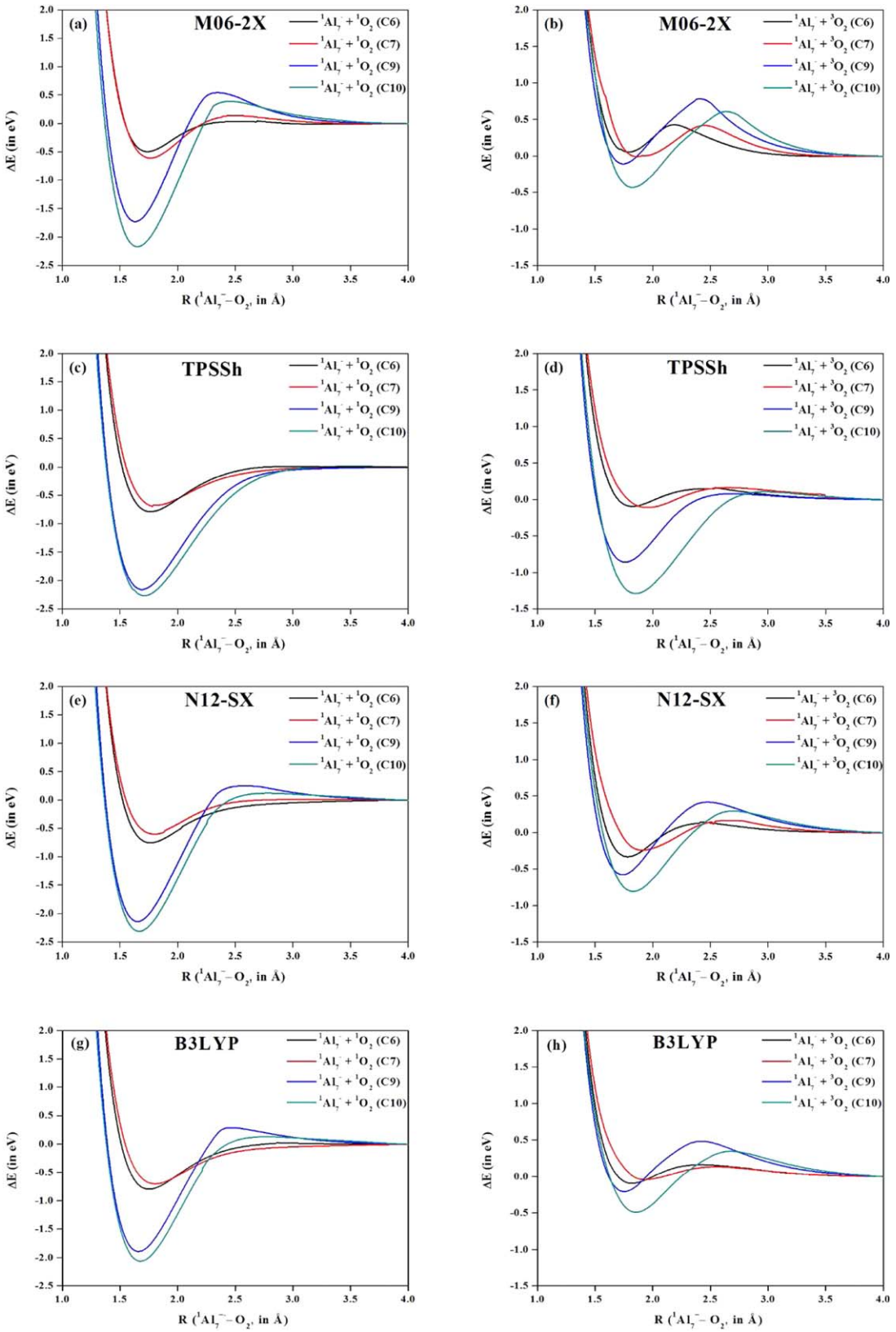

Figure 4. PESs of the reaction of O_2 with Al_7^- calculated by various DFT functionals for O_2 in a parallel orientation approaching from the top of the Al cluster (C6), O_2 in a perpendicular orientation approaching from the top of the Al cluster (C7), O_2 in a parallel orientation approaching from the side of the Al cluster (C9), and O_2 in a perpendicular orientation approaching from the side of the Al cluster (C10). Both singlet and triplet spin states were considered for O_2.

Table 3. Calculated barrier energies (in eV) for the four selected configurations calculated with M06-2X, TPSSh, N12-SX, and B3LYP functionals.

$^1Al_7^- + {}^1O_2$	C6	C7	C9	C10
M06-2X	0.04 [0.06][a]	0.13 [0.16][a]	0.54 [0.57][a]	0.31 [0.33][a]
TPSSh	0.01	0.01	0.00	0.02
N12-SX	0.00	0.01	0.25	0.12
B3LYP	0.02	0.00	0.29	0.13
CCSD(T)	0.20 [0.28][a]	0.55 [0.69][a]	0.15 [0.24][a]	0.29 [0.41][a]
$^1Al_7^- + {}^3O_2$	C6	C7	C9	C10
M06-2X	0.43 (0.39, *0.44*) [0.50][a]	0.42 (0.29, *0.29*) [0.45]	0.79 (0.25, *0.24*)[b] [0.81][a]	0.59 (0.28, *0.28*)[b] [0.61][a]
TPSSh	0.15 (0.14)[b]	0.16 (0.15)[b]	0.08 (0.08)[b]	0.11 (0.09)[b]
N12-SX	0.15 (0.15)[b]	0.17 (0.16)[b]	0.42 (0.17)[b]	0.30 (0.18)[b]
B3LYP	0.16 (0.14)[b]	0.13 (0.13)[b]	0.49 (0.20)[b]	0.35 (0.22)[b]
CCSD(T)	0.99 (0.79, *0.87*)[b] [1.15][a]	0.92 (0.37, *0.37*)[b] [1.06][a]	1.26 (1.11, 1.*11*)[b] [1.35][a]	N/A[c]

Values in parentheses are the difference in barrier energies between singlet and triplet spin states. [a] Values in square brackets are the BSSE-corrected barrier heights. [b] Values (in Italic) in parentheses are the difference in (BSSE corrected) barrier energies between singlet and triplet spin states. [c] The energy did not converge in the iteration step of the CCSD calculation.

5, the oscillating behavior of the O–O bond length within 2 Å is observed in all the ADMP trajectories. After the oscillation, the bond length of O_2 increases above 2 Å abruptly, indicating the dissociation of O_2. Thus, we consider that the dissociation of O_2 takes place when the bond length of O_2 exceeds 2 Å.

Previous experimental study on the reaction of O_2 with anion valence electrons do not react. According to our ADMP simulation results shown in Figure 5, the dissociation of O_2 on the Al cluster takes place for O_2 in both singlet and triplet spin states. However, the DFT calculations gave contrasting results on the reactivity of O_2 with the Al cluster. The M06-2X functional gave the results that are in good agreement with the experimental observation. For instance, for seven configurations (C1, C2, C7, C8, C9, C10, and C14, see Fig. 1), O_2 in the singlet spin state reacted with the Al_7^- cluster within 400 fs. In contrast, for only two configurations (C1 and C2), O_2 in the triplet spin state reacted within 400 fs. In addition, complete dissociation of O_2 in the triplet state required much longer simulation time (>250 fs). Thus, the triplet state of O_2 is less reactive than the singlet state. Contrary to M06-2X, TPSSh and N12-SX gave the results that are not consistent with the experimental observation. For example, for some configurations (C1, C9, and C10 for TPSSh, C7 and C9 for N12-SX), O_2 in the triplet state reacted in less than 200 fs. These inconsistencies can be ascribed to the underestimation of barrier height by TPSSh and N12-SX (see the previous section on the barrier energy). The difference in barrier energies between singlet and triplet states predicted by M06-2X was ~0.3 eV while the values predicted by other DFT functionals are much smaller, thus accounting for the low reactivity of O_2 in the triplet state

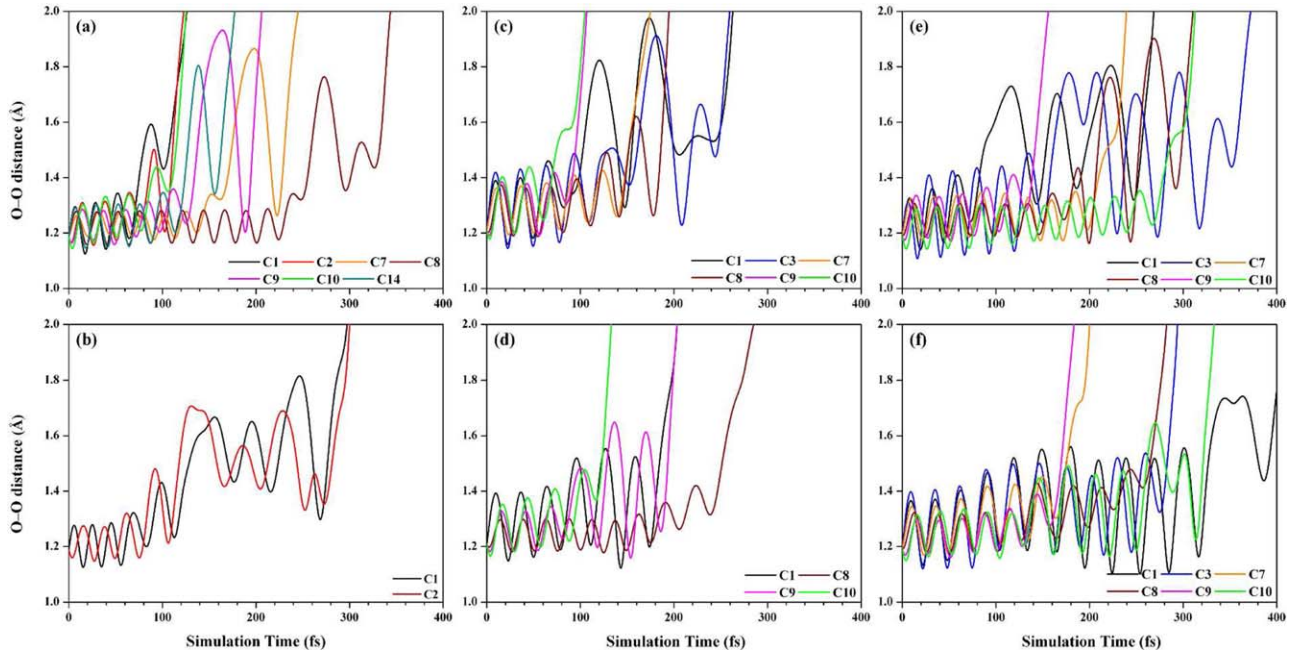

Figure 5. ADMP trajectories of the reaction of O_2 with Al_7^- calculated by the M06-2X (a) singlet and b) triplet), TPSSh (c) singlet and d) triplet), and N12-SX functionals (e) singlet and f) triplet).

predicted by the M06-2X functional. Thus, the ADMP simulation gave the results consistent with those obtained from the calculation of PESs.

The reactivity of O_2 with Al clusters may depend on the starting configuration of O_2 and Al clusters as well as the simulation time. In the present work, we examined the reactivity starting from a limited number (16) of configurations and the simulation time was only 400 fs. However, despite the limited number of starting configurations and the short simulation time, our ADMP simulation using M06-2X well reproduced the experimental observation. Therefore, the ADMP simulation with a relevant DFT functional can serve as a robust tool for examining the reactivity of sub-nanoscale materials.

Conclusions

We investigated the reactivity of O_2 on Al surfaces by performing the DFT calculation and the ADMP simulation on the model system O_2 with the Al_7^- cluster using the M06-2X, TPSSh, N12-SX, and B3LYP functionals. These four DFT functionals well describe the characteristics of charge transfer involved in the O_2/Al reactions. We observed significant structural changes and charge transfer from Al cluster to O_2 for the DS and UDS complexes. The ADMP simulations using M06-2X suggest that the O_2 in the singlet state ($^1O_2$) readily reacts with Al clusters but O_2 in the triplet state ($^3O_2$) is less reactive, which is in agreement with the experimental observation. The reproducibility of the experimental observation by the ADMP simulation is governed by the ability of a DFT functional to predict the barrier height. The M06-2X functional gave the barrier height closest to the one calculated by CCSD(T). The TPSSh functional significantly underestimated the barrier heights, presumably due to the lack of the ability to describe the charge transfer character appropriately. The M06-2X functional can be useful for studying the reaction systems between O and Al. We believe that the present work will stimulate further studies on the reactivity of O_2 with Al clusters, especially for Al-containing nanoscale systems, using computationally economical DFT methods.

Keywords: aluminum clusters · density functional theory · potential energy surface · barrier energy · ADMP simulation

How to cite this article: S. Paranthaman, J. Moon, K. Hong, J. Kim, D. E. Kim, J. Kim, T. K. Kim. *Int. J. Quantum Chem.* **2016**, *116*, 547–554. DOI: 10.1002/qua.25080

Additional Supporting Information may be found in the online version of this article.

[1] M. F. Jarrold, J. E. Bower, *Chem. Phys. Lett.* **1988**, *144*, 311.
[2] J. Jacobsen, B. Hammer, K. W. Jacobsen, J. No, *Phys. Rev. B* **1995**, *52*, 14954.
[3] F. Libisch, C. Huang, P. Liao, M. Pavone, E. A. Carter, *Phys. Rev. Lett.* **2012**, *109*, 198303.
[4] R. Leuchtner, A. Harms, A. Castleman, Jr., *J. Chem. Phys.* **1991**, *94*, 1093.
[5] R. Burgert, H. Schnöckel, A. Grubisic, X. Li, S. T. Stokes, K. H. Bowen, G. Ganteför, B. Kiran, P. Jena, *Science* **2008**, *319*, 438.
[6] W. H. Woodward, N. Eyet, N. S. Shuman, J. C. Smith, A. A. Viggiano, A. Castleman, Jr., *J. Phys. Chem. C* **2011**, *115*, 9903.
[7] H. Brune, J. Wintterlin, R. Behm, G. Ertl, *Phys. Rev. Lett.* **1992**, *68*, 624.
[8] L. Österlund, I. Zoric-Acute, B. Kasemo, *Phys. Rev. B* **1997**, *55*, 15452.
[9] C. Mosch, C. Koukounas, N. Bacalis, A. Metropoulos, A. Gross, A. Mavridis, *J. Phys. Chem. C* **2008**, *112*, 6924.
[10] Q. Yuan, J. Li, X. Fan, W. Lau, Z. F. Liu, *Chem. Phys. Lett.* **2010**, *489*, 16.
[11] T. Sasaki, T. Ohno, *Surf. Sci.* **1999**, *433*, 172.
[12] Y. F. Zhukovskii, P. Jacobs, M. Causá, *J. Phys. Chem. Solids* **2003**, *64*, 1317.
[13] K. Honkala, K. Laasonen, *Phys. Rev. Lett.* **2000**, *84*, 705.
[14] Y. Yourdshahyan, B. Razaznejad, B. I. Lundqvist, *Phys. Rev. B* **2002**, *65*, 075416.
[15] N. Bacalis, A. Metropoulos, A. Gross, *J. Phys. Chem. A* **2010**, *114*, 11746.
[16] H. R. Liu, H. Xiang, X. G. Gong, *J. Chem. Phys.* **2011**, *135*, 214702.
[17] N. C. Bacalis, A. Metropoulos, A. Gross, *J. Phys. Chem. C* **2012**, *116*, 16430.
[18] H. B. Schlegel, J. M. Millam, S. S. Iyengar, G. A. Voth, A. D. Daniels, G. E. Scuseria, M. J. Frisch, *J. Chem. Phys.* **2001**, *114*, 9758.
[19] S. S. Iyengar, H. B. Schlegel, J. M. Millam, G. A Voth, G. E. Scuseria, M. J. Frisch, *J. Chem. Phys.* **2001**, *115*, 10291.
[20] H. B. Schlegel, S. S. Iyengar, X. Li, J. M. Millam, G. A. Voth, G. E. Scuseria, M. J. Frisch, *J. Chem. Phys.* **2002**, *117*, 8694.
[21] Y. Zhao, D. G. Truhlar, *Theor. Chem. Acc.* **2008**, *120*, 215.
[22] V. N. Staroverov, G. E. Scuseria, J. Tao, J. P. Perdew, *J. Chem. Phys.* **2003**, *119*, 12129.
[23] R. Peverati, D. G. Truhlar, *Phys. Chem. Chem. Phys.* **2012**, *14*, 16187.
[24] S. Paranthaman, K. Hong, J. Kim, D. E. Kim, T. K. Kim, *J. Phys. Chem. A* **2013**, *117*, 9293.
[25] V. O. Kiohara, E. F. Carvalho, C. W. Paschoal, F. B. Machado, O. Roberto-Neto, *Chem. Phys. Lett.* **2013**, *568*, 42.
[26] A. D. Becke, *Phys. Rev. A* **1988**, *38*, 3098.
[27] C. Lee, W. Yang, R. G. Parr, *Phys. Rev. B* **1988**, *37*, 785.
[28] A. E. Reed, L. A. Curtiss, F. Weinhold, *Chem. Rev.* **1988**, *88*, 899.
[29] K. Raghavachari, G. W. Trucks, J. A. Pople, M. Head-Gordon, *Chem. Phys. Lett.* **1989**, *157*, 479.
[30] S. F. Boys, F. Bernardi, *Mol. Phys.* **1970**, *19*, 553.
[31] G. W. T. M. J. Frisch, H. B. Schlegel, G. E. Scuseria, M. A. Robb, J. R. Cheeseman, G. Scalmani, V. Barone, B., G. A. P. Mennucci, H. Nakatsuji, M. Caricato, X. Li, H. P. Hratchian, A. F. Izmaylov, J. Bloino, G. Zheng, J. L. Sonnenberg, M. Hada, M. Ehara, K. Toyota, R. Fukuda, M. I. J. Hasegawa, T. Nakajima, Y. Honda, O. Kitao, H. Nakai, T. Vreven, J. A. Montgomery, Jr., J. E. Peralta, F. Ogliaro, M. Bearpark, J. J. Heyd, E. Brothers, K. N. Kudin, V. N. Staroverov, R. Kobayashi, J. Normand, K. Raghavachari, A. Rendell, J. C. Burant, S. S. Iyengar, J. Tomasi, M. Cossi, N. Rega, J. M. Millam, M. Klene, J. E. Knox, J. B. Cross, V. Bakken, C. Adamo, J. Jaramillo, R. Gomperts, R. E. Stratmann, O. Yazyev, A. J. Austin, R. Cammi, C. Pomelli, J. W. Ochterski, R. L. Martin, K. Morokuma, V. G. Zakrzewski, G. A. Voth, P. Salvador, J. J. Dannenberg, S. Dapprich, A. D. Daniels, C. Farkas, J. B. Foresman, J. V. Ortiz, J. Cioslowski, D. J. Fox, In Gaussian 09 (Revision D.01); Gaussian, Inc.: Wallingford, CT, **2009**.
[32] N. Drebov, F. Weigend, R. Ahlrichs, *J. Chem. Phys.* **2011**, *135*, 044314.
[33] K. P. Huber, G. Herzberg, Constants of Diatomic Molecules; Van Nostrand Reinhold: New York **1979**, 534.
[34] O. Launila, J. Jonsson, *J. Mol. Spectrosc.* **1994**, *168*, 1.
[35] B. Lengsfield III, B. Liu, *J. Chem. Phys.* **1982**, *77*, 6083.
[36] L. Andrews, T. R. Burkholder, J. T. Yustein, *J. Phys. Chem.* **1992**, *96*, 10182.

Received: 5 October 2015
Revised: 11 December 2015
Accepted: 21 December 2015
Published online 20 January 2016